

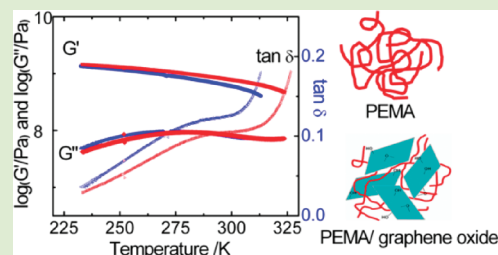
Considering Viscoelastic Micromechanics for the Reinforcement of Graphene Polymer Nanocomposites

Xiguang Li and Gregory B. McKenna*

Department of Chemical Engineering, Whitacre College of Engineering, Texas Tech University, Lubbock, Texas 79409-4121, United States

ABSTRACT: There has been much recent work investigating the reinforcement of glassy polymers with nanoparticles, and much excitement has been generated by some apparent synergies that suggest reinforcements greater than expected from elastic bound models. Here we show that it is necessary to consider the thermoviscoelastic response of the polymer matrix in nanocomposites (PNCs) to fully understand the reinforcement of the filler. This is especially so because polymer nanocomposites are frequently used at high fractions of the glass transition temperature T_g , where the time dependence of the polymer is significant. Therefore it is a conceptual error to examine the modulus behavior of PNCs via only elastic micromechanics.

When the glass transition temperature increases due to the interactions between reinforcement and polymer, it is more reasonable to use a viscoelastic micromechanics approach to estimate the bounds on modulus behavior of PNCs. Here we use new results for graphene oxide reinforced poly(ethyl methacrylate) (PEMA) and literature results for reinforced poly(methyl methacrylate) (PMMA) and show that the ultralow loading of graphene oxide raises the T_g of PEMA and PMMA significantly and leads to a large shift of the frequency–temperature properties of the polymer matrix. Our thermoviscoelastic approach shows that apparent extreme reinforcements can be attributed to the changing T_g of the polymer, and the corrected mechanical reinforcement from graphene oxide is much weaker than previously reported.



Recently, it has been reported^{1–3} that dispersing graphene or graphene oxide into polymer matrices at ultralow loadings (<0.50 vol %) can lead to excellent mechanical reinforcement of polymer nanocomposites (PNCs). In some instances, such as PMMA/graphene oxide (33% enhancement of Young's modulus E at only 0.005 vol %),¹ results were interpreted to exceed the idealized Voigt upper bound prediction (the limit of infinite aspect ratio of filler and perfect alignment).^{5,9} The Halpin–Tsai model prediction⁷ has also been exceeded in an epoxy/graphene system (31% increment of Young's modulus at 0.05 vol %).³ The authors attributed this high reinforcement to a hydrogen-bonding interaction¹ or an enhanced nanofiller-polymer mechanical interlocking due to the wrinkled morphology of graphene.^{1,3} These striking results exceeding elastic micromechanics predictions lead to a great enthusiasm for the prospect of graphene polymer nanocomposites. At the same time, Kim et al. have questioned these surprising results and the associated explanations.⁶

An interesting phenomenon to be considered in what follows is that associated with the reported striking reinforcement is a significant increase in the glass transition temperature (T_g): 17 K at 0.005 vol % (PMMA/graphene oxide)¹ and 10 K at 0.05 vol % (epoxy/graphene).^{3,4} In Figure 1, constructed from Ruoff's data,² one can see that the increase of T_g and reinforcement for PMMA/graphene oxide nanocomposites share a similar trend. This hint that T_g and modulus increases are correlated leads us to consider that the thermoviscoelasticity of the polymer matrix changes with the addition of the graphene or graphene oxide, and we propose that incorporation of viscoelastic

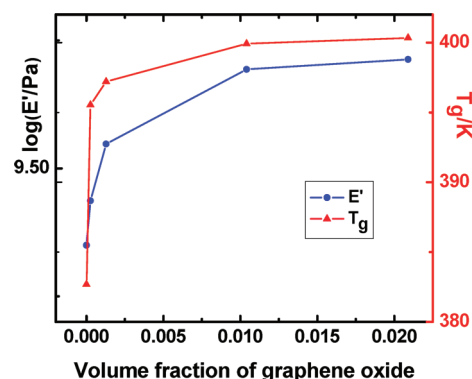


Figure 1. Glass transition temperature and storage tensile modulus E' of PMMA/graphene oxide at 313 K versus graphene oxide loading (data from ref 2).

micromechanics rather than conventional elastic micromechanics is necessary to describe the reinforcement of PNCs especially if the T_g of the matrix is changed by the addition of a nanofiller. As shown below, apparently high reinforcement can be attributed to the changing thermoviscoelasticity of the polymer matrix.

The most widely used elastic micromechanics theories are the Voigt upper bound mixing rule,⁵ Halpin–Tsai equation,⁷

Received: December 31, 2011

Accepted: February 20, 2012

Published: February 27, 2012

and Mori–Tanaka model,⁸ and they are used to predict elastic properties of composites.^{9,10} To account for the polymer matrix viscoelasticity in composite materials, Hashin defined a viscoelastic micromechanics model for the modulus behavior^{11,12}

$$E_c^*(i\omega) = V_m E_m^*(i\omega) + V_f E_f$$

$$E_m^*(i\omega) = E_m'(\omega) + iE_m''(\omega) \quad (1)$$

where E^* is the complex modulus; V is the volume fraction of components; subscripts are m for the polymer matrix, f for filler, and c for composite.

In the present letter, we examine the influence of viscoelasticity of the polymer matrix on the PNCs reinforcement and especially consider changes in the viscoelastic properties induced by the changing T_g upon graphene oxide addition. We provide new experimental results for the glass transition and complex modulus of poly(ethyl methacrylate)/graphene oxide nanocomposites (PEMAGO) and consider literature data² for poly(methyl methacrylate)/graphene oxide nanocomposites (PMMAGO). A thermoviscoelastic micromechanics approach is presented to explain the reinforcement of graphene polymer nanocomposites.

Graphene oxide was exfoliated from graphite oxide (purchased from Graphene Laboratories, Inc.) by ultrasonication using a Misonix sonicator (XL 2000), then mixed with PEMA (purchased from Sigma-Aldrich, $M_w = 515$ kg/mol) using a solution-mixing procedure.¹ The graphene oxide was added to the system as 0.25 wt % or 0.12 vol %. Rectangular bar samples ($1.3 \times 8.0 \times 45$ mm³) and cylindrical samples (8.0 mm diameter, 1.1 mm height) were prepared through compression molding using a hot-press at 453 K. Dynamic mechanical properties were characterized using an ARES rheometer with a rectangular torsion fixture (from 230 to 330 K) and parallel plate fixture (from 330 to 370 K). The glass transition temperature T_g was determined as the limiting fictive temperature¹³ T_f' , measured by a TA Q20 differential scanning calorimeter (DSC) by heating at 10 K/min after cooling at 10 K/min.

As seen in Table 1 and Figure 2, a significant increase in the glass transition temperature T_g (nearly 15 K) was observed for

Table 1. Glass Transition Temperature of PEMA and PEMAGO

method	PEMA	0.12 vol % PEMAGO	ΔT_g
DSC	337.4 K	352.2 K	14.8 K
rheometry (by the loss modulus G'' peak location in Figure 2)	334.6 K	350.8 K	16.2 K

the 0.12 vol % PEMAGO. This could be attributed to hydrogen bonding between graphene oxide and the carbonyl groups of PEMA, leading to a strong interaction of graphene oxide with the PEMA, as postulated for the PMMA/graphene system.¹ This is also similar to the increased T_g values that have been reported in thin polymer films on substrates with strong interactions,¹⁴ such as PMMA on native silicon oxide.¹⁵

Figure 3 shows dynamic temperature ramp results for both the PEMAGO from this work and the PMMAGO from ref 2. The addition of graphene oxide causes a shift in the curves toward higher temperatures for both materials, consistent with a nearly 15 K increment in T_g for the PEMAGO 0.12 vol %, 14 K for the PMMAGO 0.13 vol %, and 17 K for the PMMAGO

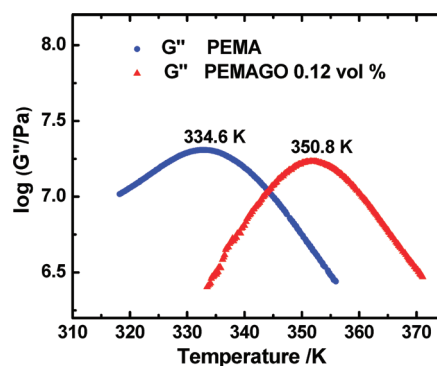


Figure 2. Loss modulus versus temperature for PEMA and PEMAGO 0.12 vol % from 320 to 370 K (heating rate at 1 K/min; $\omega = 6.28$ rad/s; strain is 0.02%).

1.0 vol %. Therefore, the polymer matrix with the graphene oxide seems to behave as the pure polymer at lower temperatures, showing the importance of the matrix thermoviscoelasticity. In addition, we can see for the PEMA peak of the loss shear modulus G'' , there is little change in the strength of the β relaxation, which means the graphene oxide does not reinforce the PEMA as an antiplastizer.¹⁶

Dynamic frequency sweep results for the PEMA and PEMAGO at different temperatures are shown in Figure 4. At 298 K (room temperature), the curves for G' and G'' for the 0.12 vol % PEMAGO (solid square and solid diamond) overlap the curves of pure PEMA at 283 K (open circle and open triangle), which is consistent with the increase of 15 K in the T_g and for the frequency–temperature behavior of the polymer matrix.

To further explore the influence of the matrix thermoviscoelasticity and elasticity on the reinforcement for graphene polymer nanocomposites, the dynamic temperature ramp data were shifted to the same value of $T - T_g$ in Figure 5. It is found that for the PEMA the curves for storage modulus G' coincide well though the loss modulus curves do not overlap well due to the β relaxation¹⁷ (Figure 5a). In the case of the PMMA, it is found that E' and E'' for the PMMAGO 0.13 vol % nearly overlap the PMMA curves, but the PMMAGO 1.0 vol % shows a slight vertical shift (Figure 5b).

The apparent experimental reinforcements can be obtained using eq 2 for the data of Figure 3. However, upon considering the thermoviscoelasticity, eq 2 was modified to eq 3 by replacing the modulus as function of temperature by the modulus as function of $T - T_g$, to give corrected experimental reinforcements from the shifted data of Figure 5. In a similar manner the reinforcement prediction from the elastic Voigt upper bound (eq 4) was modified to the viscoelastic Voigt upper bound (eq 5).

$$\frac{E_c(T)}{E_m(T)} - 1 \quad (2)$$

$$\frac{E_c(T - T_g)}{E_m(T - T_g)} - 1 \quad (3)$$

$$\frac{V_m E_m(T) + V_f E_f}{E_m(T)} - 1 \quad (4)$$

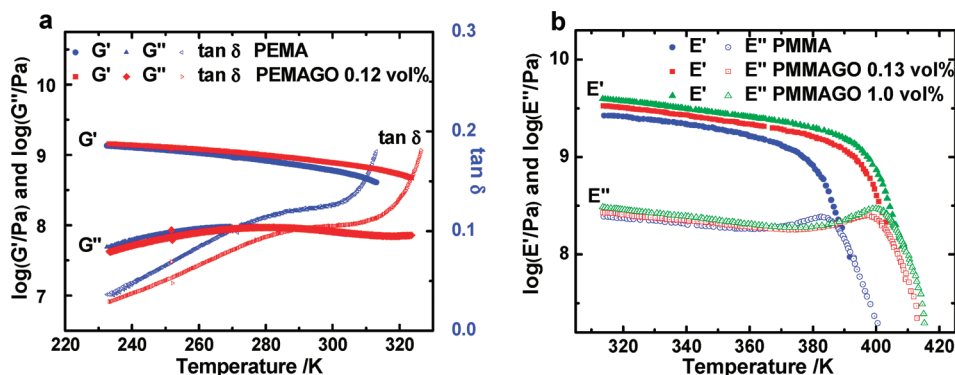


Figure 3. Loss and storage moduli during temperature ramp for (a) PEMA and PEMAGO 0.12 vol % from 230 to 330 K (heating rate at 1 K/min; $\omega = 6.28$ rad/s; strain is 0.02%) and (b) PMMA and PMMAGO (data from ref 2).

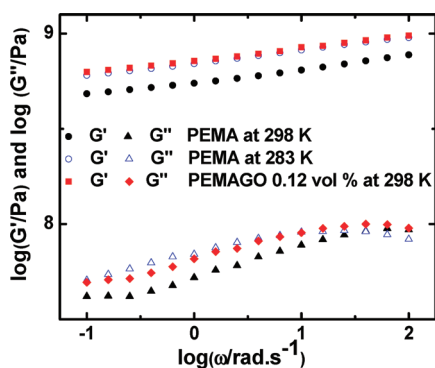


Figure 4. Dynamic frequency sweep of PEMA and PEMAGO 0.12 vol % at 283 and 298 K (strain is 0.02%).

$$\frac{V_m E_m (T - T_g) + V_f E_f}{E_m (T - T_g)} - 1 \quad (5)$$

It is worth noting that the interest in the Voigt bounds arises because properties that exceed these bounds are considered to be evidence for “extreme reinforcement” or synergistic reinforcement, which could be evidence for novel behavior in such nanocomposites.

The influence of viscoelasticity is more clearly illustrated in Figure 6, where the apparent experimental reinforcements (obtained by eq 2) are plotted for different temperatures and compared to the elastic Voigt upper bound predictions (eq 4). The corrected reinforcements obtained from eq 3 are also shown to compare with the viscoelastic Voigt upper bound pre-

dictions (from eq 5) in Figure 6. Although the apparent uncorrected reinforcement is close to or even exceeds the elastic Voigt upper bound prediction, it is clear that the corrected reinforcements are much weaker than the viscoelastic upper bound prediction.

Figure 6 demonstrates that in polymer nanocomposites, the apparent reinforcement can be attributed to the changed viscoelasticity of the polymer induced by the T_g change. The corrected effect of the graphene oxide reinforcement on PEMA and PMMA at ultralow loading is not as high as has been reported and accounting for the viscoelastic response indicates less reinforcement than estimated from the elastic bound, hence providing a reason to Kim et al.'s skepticism concerning claims of extreme reinforcement. It may also explain Ruoff's work with polycarbonate/graphene oxide that exhibits weak reinforcement, where little T_g change is seen.¹⁸

The results presented here show that it is necessary to consider the thermoviscoelastic response of the polymer matrix in nanocomposites (PNCs) to fully understand the reinforcement of the filler. This is especially so because polymer nanocomposites are frequently used at high fractions of the T_g , where the time dependence of the polymer is significant.¹⁹ Therefore it is a conceptual error to examine the modulus behavior of PNCs via only elastic micromechanics. When the glass transition temperature increases, the polymer matrix in the PNCs behaves as the pure polymer at a lower temperature, contradicting the inherent assumption in elastic micromechanics. Consequently, it is more reasonable to use Hashin's viscoelastic micromechanics model, taking into account changes in matrix response due to the addition of the filler, to estimate

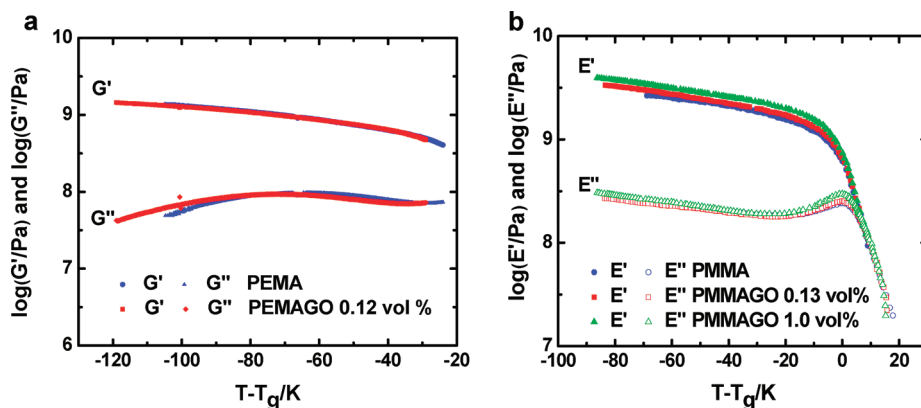


Figure 5. Storage modulus and loss modulus versus $T - T_g$ of (a) PEMA and PEMAGO 0.12 vol % and (b) PMMA and PMMAGO (data from ref 2).

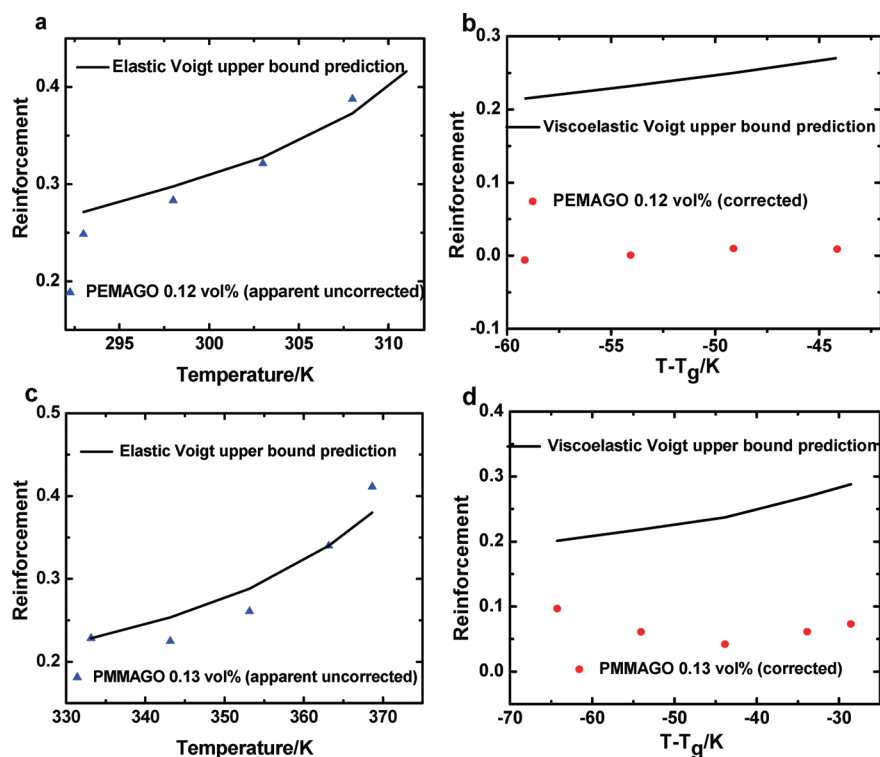


Figure 6. Apparent and corrected reinforcements and Voigt upper bound predictions for (a, b) PEMAGO 0.12 vol % ($\omega = 6.28$ rad/s) and (c, d) PMMAGO 0.13 vol % ($f = 1$ Hz) (data from ref 2).

the bounds on modulus behavior of PNCs.^{11,12} At temperatures much farther below T_g or when there is no change of T_g , the changes in the viscoelasticity of the polymer matrix are less important, and the elastic micromechanics might be considered to capture the approximate reinforcement behavior of PNCs.

In summary, we have demonstrated that the ultralow loading of graphene oxide raises the T_g of PEMA and PMMA significantly and leads to a large shift of the frequency–temperature properties of the polymer matrix. In such a condition, it is necessary to consider the influence of thermoviscoelasticity on the expected reinforcement in graphene oxide polymer nanocomposites, and Hashin's viscoelastic micromechanics should be considered. Our thermoviscoelastic approach shows that apparent extreme reinforcements can be attributed to the changing T_g of the polymer, and the corrected mechanical reinforcement from graphene oxide is much weaker than previously reported.

AUTHOR INFORMATION

Corresponding Author

*E-mail: greg.mckenna@ttu.edu.

Notes

The authors declare no competing financial interest.

ACKNOWLEDGMENTS

The authors acknowledge the John R. Bradford Endowment at Texas Tech University and the National Science Foundation under grant CHE-1112416 both for partial support of this work.

REFERENCES

(1) Ramanathan, T.; Abdala, A. A.; Stankovich, S.; Dikin, D. A.; Herrera-Alonso, M.; Piner, R. D.; Adamson, D. H.; Schniepp, H. C.;

Chen, X.; Ruoff, R. S.; Nguyen, S. T.; Aksay, I. A.; Prud'Homme, R. K.; Brinson, L. C. *Nat. Nanotechnol.* **2008**, *3*, 327–331.

(2) Potts, J. R.; Lee, S. H.; Alam, T. M.; An, J.; Stoller, M. D.; Piner, R. D.; Ruoff, R. S. *Carbon* **2011**, *49*, 2615–2623.

(3) Rafiee, M. A.; Rafiee, J.; Wang, Z.; Song, H.; Yu, Z.-Z.; Koratkar, N. *ACS Nano* **2009**, *3*, 3884–3890.

(4) Yavari, F.; Rafiee, M. A.; Rafiee, J.; Yu, Z.-Z.; Koratkar, N. *ACS Appl. Mater. Interfaces* **2010**, *2*, 2738–2743.

(5) Liu, B.; Feng, X.; Zhang, S. *Compos. Sci. Technol.* **2009**, *69*, 2198–2204.

(6) Kim, H.; Abdala, A. A.; Macosko, C. W. *Macromolecules* **2010**, *43*, 6515–6530.

(7) Halpin, J. C. *J. Compos. Mater.* **1969**, *3*, 732–734.

(8) Mori, T.; Tanaka, K. *Acta Metall.* **1973**, *21*, 571–574.

(9) Fornes, T. D.; Paul, D. R. *Polymer* **2003**, *44*, 4993–5013.

(10) Tucker, C. L.; Liang, E. *Compos. Sci. Technol.* **1999**, *59*, 655–671.

(11) Hashin, Z. *J. Appl. Mechanics* **1965**, *32*, 630–636.

(12) Hashin, Z. *Int. J. Solids Struct.* **1970**, *6*, 797–807.

(13) Badrinarayanan, P.; Zheng, W.; Li, Q.; Simon, S. L. *J. Non-Cryst. Solids* **2007**, *353*, 2603–2612.

(14) Alcoutlabi, M.; McKenna, G. B. *J. Phys.: Condens. Matter* **2005**, *17*, 461–524.

(15) Keddie, J. L.; Jones, R. A. L.; Cory, R. A. *Faraday Discuss.* **1994**, *98*, 219–230.

(16) Robeson, L. M.; Faucher, J. A. *Polym. Lett.* **1969**, *7*, 35–40.

(17) Kulik, A. S.; Beckham, H. W.; Schmidt-Rohr, K.; Radloff, D.; Pawelzik, U.; Boeffel, C.; Spiess, H. W. *Macromolecules* **1994**, *27*, 4746–4754.

(18) Potts, J. R.; Murali, S.; Zhu, Y.; Zhao, X.; Ruoff, R. S. *Macromolecules* **2011**, *44*, 6488–6495.

(19) McKenna, G. B. Dynamics of materials at the nanoscale. In *Polymer Physics: From suspensions to nanocomposites and beyond*; Utracki, L. A., Jamieson, A. M., Eds.; Wiley: New York, 2010; Chapter 5, pp 191–223.